2.3 Devices: Photovoltaic cells, light emitting diodes and field-effect transistors

Finally, the effects discussed in the previous chapters will be used in the discussion of devices, mainly photovoltaic cells, light emitting diodes and field-effect transistors.
Refs. [K. Seeger "Semiconductor Physics", 2004, Springer Verlag], [H. Lueth "Solid surfaces, interfaces and thin film", 2010, Springer], [J. Nelson, "Optics and Solar Energy", Imperial College London (Lecture notes)], [E. F. Schubert "Light emitting diodes" Cambridge University Press (2006)]

2.3.1 Solar cells

The radiant power of the sun at the earth's surface is about 100000TW, which is 50000 times more than the power consumption of the entire population. This makes the conversion of solar radiation into electricity an obvious way to solve or at least reduce the energy crisis.
The working principle of a solar cell is based on the photovoltaic effect, which describes the generation of free charge carriers after absorption of a photon with an energy $h\nu$ higher than the optical gap E_G of the material ($h\nu > E_G$). If the charge carriers are generated at a potential barrier (e.g. a pn-junction), a photovoltaic potential is generated, which leads to a measurable current.
The simplest solar cell structure is a metallic grid as front electrode, a pn-junction as active layer and a back electrode. Usually, an anti-reflective coating is placed between grid and active layer to increase the transmission.

2.3.1.1 Working principle

In the following we will briefly discuss some processes in solar cells.

1) Absorption of light and creation of electron-hole pairs
If the photon energy is equal or larger than the band gap (in case of direct band gap semiconductors), electrons are excited from the valence band into the conduction band under illumination, leaving holes in the valence band behind. These optically excited Coulombically bound electron-hole pairs are called excitons. Their binding energy is given by the distance of the electron-hole pair and the dielectric constant of the surrounding medium (the crystal, e.g.) and has to be overcome in order to obtain free charge carriers. In inorganic semiconductors, the exciton binding energy is in the order of 10meV, i.e. the separation of the exciton into free charge carriers can be easily achieved.
The generation rate of electron hole pairs per cm^3 per second depends on the wavelength λ of the absorbed photon, the incident photon flux $f(\lambda)$ (i.e. number of photons per area per second per λ), the absorption coefficient $\alpha(\lambda)$, the reflectance $r(\lambda)$ and lastly, the grid shadowing factor s:

$$G = (1-s)\int_{\lambda}(1-r(\lambda))f(\lambda)e^{-\alpha\lambda}\alpha(\lambda)d\lambda \tag{2.35}$$

Here, the absorption coefficient $\alpha(h\nu) \propto P_{12} g_v(E_1) g_c(E_1)$ depends on the photo energy $h\nu$, the probability of the transition P_{12}, given by Fermi's Golden Rule, and the electron densities of the initial ($g_v(E_1)$) and final ($g_c(E_1)$) states.

2) Separation of electron-hole pairs, carrier transport
Due to the electric field at the interface of the pn-junction caused by the built-in potential U_D or V_{bi}(see Chapter 2.2, p. 40), the electron-hole pair is separated and the free charge carriers diffuse to the electrodes, where they are collected.
The current density of a solar cell is dominated by minority charge carrier diffusion and can be described by continuity equations for electrons and holes:

$$\vec{\nabla} \cdot \vec{j}_n = q(-G + R_n + \frac{\partial n}{\partial t}) \tag{2.36}$$

and

$$\vec{\nabla} \cdot \vec{j}_p = q(G - R_p - \frac{\partial p}{\partial t}) \tag{2.37}$$

with G the generation rate of electron-hole pairs discussed before, R the recombination rate discussed below and $\frac{\partial n/p}{\partial t}$ the change in electron n or hole p concentrations.

3) Loss mechanisms: Recombination
The radiative or non-radiative recombination of an electron-hole pair is an obvious loss mechanism in a solar cell. There are several recombination channels possible:

- Recombination via trap states, which depends on the capture cross-section, the velocity of the charge carriers and the density of trap states
- Radiative recombination, which depends on the density of charge carriers
- Auger recombination, which is similar to the radiative recombination with the difference that the excitation energy is given to another charge carrier which then relaxes thermally (via phonons)
- Recombination via surface states (similar to recombination via trap states)

2.3.1.2 Current voltage characteristics, figures of merit

Important parameters are:

- The open circuit voltage V_{OC}
- The short circuit current I_{SC}
- The maximum power point MP given by $V_{MP} \cdot I_{MP} = max.$

With these parameters, we can define some figures of merit:

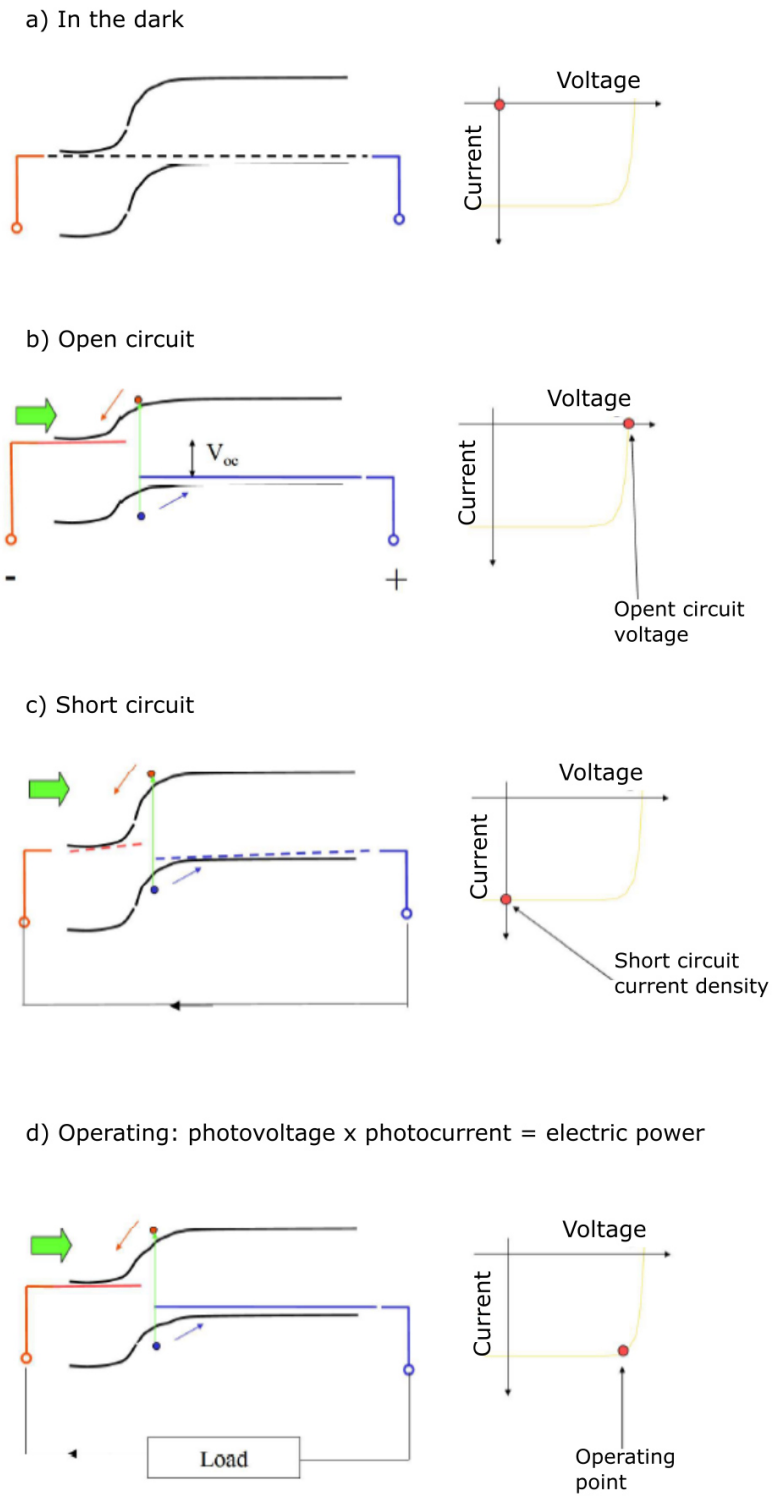

Fig. 2.12: Figures of merit of a solar cell. Important parameters are the open circuit voltage V_{OC}, the short circuit current I_{SC} and the maximum power point MP given by $V_{MP} \cdot I_{MP} = max.$. (Figures from J. Nelson, "Optics and Solar Energy", Imperial College London (Lecture notes)).

- The **fill factor** is: $FF = \frac{V_{MP}I_{MP}}{V_{OC}I_{SC}} = \frac{P_{MP}}{V_{OC}I_{SC}}$
- The **power conversion efficiency** is: $\eta = \frac{P_{MP}}{P_{in}}$ with P_{in} the incident power of the solar spectrum.
- The **external collection efficiency** is: $\eta_C^{ext} = \frac{I_{SC}}{Iinc}$ with I_{inc} the maximum possible photocurrent of an area A if all photons with $E > E_G$ create electron-hole pairs.
- The **internal collection efficiency** is: $\eta_C^{int} = \frac{I_{SC}}{I_{gen}}$ with I_{gen} the light generated current. This is what the short circuit current would be if every photon that is absorbed leads to charge carriers which are all extracted and contribute to the short circuit current. $I_{gen} = I_{inc}$ if there are no grid shadowing effects, no reflection losses and the solar cell is infinitely thick.

2.3.1.3 Theoretical efficiency limit (Shockley Queisser limit)

Describes the energy conversion efficiency limit ν_{ult} of a single junction solar cell with the following assumptions:

- Direct bandgap material
- For all photons with energy above the bandgap electron-hole pairs are created with $h\nu_{th} = \Delta\epsilon_{th}$
- The solar spectrum can be approximated as the spectrum of a black body

Theoretical limits for some materials:

- Silicon: 44%
- GaAl: 41%
- amorphous silicon: 37%

However:

- The real solar spectrum shows deviations from the black body radiation (due to atmospheric absorption)
- Not all photons with energies above the band gap are equally well absorbed (the absorption spectrum of the material has to be taken into account)
- Not each absorbed photon leads to an electron-hole pair that this separated and collected (see collection efficiencies)
- The charge diffusion length may determine whether electrons and holes reach the respective electrodes

Special considerations for solar cells with organic semiconductors as active layer
In recent years, solar cells based on organic semiconductors have gained increased attention. Although the general working principle is very similar there are some differences between solar cells based on inorganic and organic semiconductors:

- The dielectric constants of organic semiconductors are smaller than of inorganic semiconductors. Both, the screening length and the exciton binding energy are proportional to the dielectric constant. In particular, the fact that the binding energy is significantly higher leads to less efficient charge separation.
- A pn-junction of organic semiconductors is usually not realized via doping, but involves two different organic semiconductors, one of which then acts as donor and the other as acceptor. This strongly affects the charge separation process (with now is mainly determined by a charge transfer from one compound to the other) and the following charge transport.
- The diffusion lengths in organic semiconductors are shorter than in inorganic semiconductors due to lower structural order. Furthermore, the charge transport mechanism is different and includes hopping transport. This reduces the collection efficiency of the charge carriers.
- The main advantage of organic semiconductors is the lower process temperature and the fact that the absorption can be tuned to match the solar cell spectrum.

Improvements of solar cell efficiency
Ways to improve solar cell efficiency include:

- Optimized geometries for efficient separation of electron-hole pairs
- Tandem solar cells (made of different band gap materials) for optimized harvesting of solar photons
- Up-/Down-conversion to harvest larger range of solar spectrum

2.3.2 Light emitting diodes

2.3.2.1 Working principle

The working principle of light emitting diodes is in rough approximation reversed to that of the solar cell. While a solar cell generates electrical power by absorption of photons, the injection of charge carriers into a pn-junction leads to the emission of light in a light emitting diode (LED).
Compared to conventional lighting devices (incandescent light bulbs, fluorescent light sources, arc lamps...), LEDs are more reliable, are more efficient, can be made more compact, show fast response and emit a narrow band spectrum, which makes them extremely well suited as monochromatic light sources. The disadvantage is that several

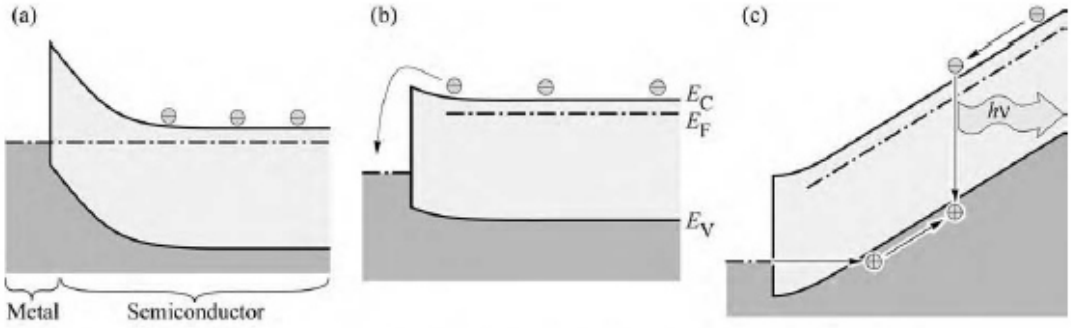

Fig. 1.2. Band diagram of a Schottky diode under (a) equilibrium conditions, (b) forward bias, and (c) strong forward bias. Under strong forward bias, minority carrier injection occurs, making possible near-bandgap light emission.

Fig. 2.13: Figure from E.F. Schubert "Light emitting diodes" Cambridge University Press (2006).

LEDs have to be combined to create white light and in particular, the creation of blue light is difficult (Nobel prize 2014).
Common materials for LEDs are crystalline Si, GaAs (also in quantum well structures with AlGaAs) and GaInP pn-junctions.

The basic principle on which any LED is based is electroluminescence, which is light emission from a solid caused by an electrical power source. Accordingly, the most crucial step in the functioning of an LED is the recombination of injected charge carriers.
So far, we discussed mainly the generation of free carriers by thermal excitation, doping or optical excitation. In LEDs, the excess free carriers are injected from the electrodes. The total carrier density is given by $n = n_0 + \Delta n$ and $p = p_0 + \Delta p$, where n_0/p_0 denote the equilibrium charge carrier density and $\Delta n/\Delta p$ the excess charge carrier densities due to injection.
Recombination leads to a decrease in the charge carrier density and the recombination rate can be written as:

$$R = -\frac{dn}{dt} = -\frac{dp}{dt} = Bnp \tag{2.38}$$

with the recombination coefficient B.
The probability that an electron and a hole recombine depends on the density of electrons and holes. Since the electrons and holes recombine in pairs (and are also injected in pairs), the steady state electron and hole densities are equal: $\Delta n(t) = \Delta p(t)$.
Apart from radiative recombination of electrons and holes under the emission of light, there are also non-radiative decay mechanisms equal to those observed in solar cells (non-radiative recombination via Auger processes, deep traps or surface states). In particular, surface recombination can significantly reduce the intensity of a LEDs.

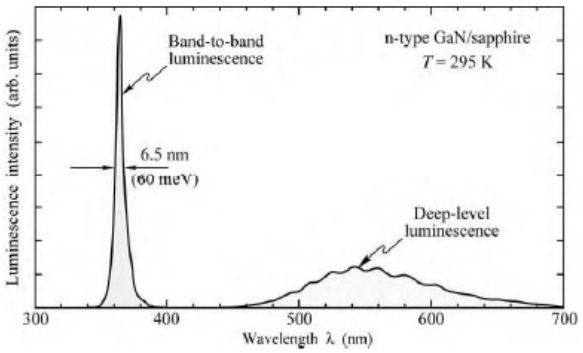

Fig. 2.8. Room-temperature photoluminescence spectrum of GaN with a band-to-band optical transition at 365 nm and a second transition at 550 nm identified as an optically active deep-level transition (after Grieshaber *et al.*, 1996).

Fig. 2.14: Figure from E.F. Schubert "Light emitting diodes" Cambridge University Press (2006).

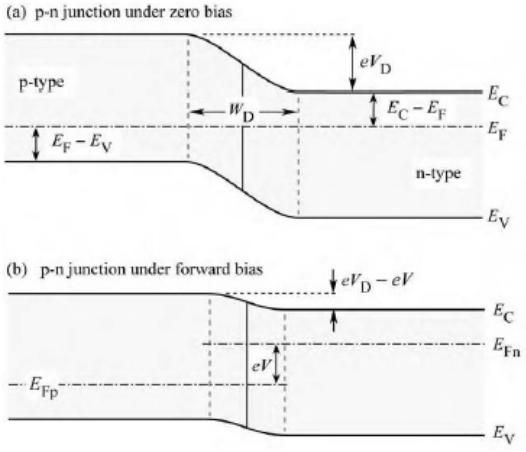

Fig. 4.1. P-n junction under (a) zero bias and (b) forward bias. Under forward-bias conditions, minority carriers diffuse into the neutral regions where they recombine.

Fig. 2.15: Figure from E.F. Schubert "Light emitting diodes" Cambridge University Press (2006).

2.3.2.2 Electrical characteristics of a light emitting diodes

In an unbiased pn-junction, electrons originating from ionized donors on the n-side diffuse to the p-side (and holes vice versa) and form the well-known space charge layer (depletion region). The charge in the depletion region is due to stationary ionized donors and acceptors and produces a built-in potential (leading to a diffusion voltage V_D).

$$V_D = \frac{k_B T}{e} ln \left(\frac{N_A N_D}{n_i^2} \right) \tag{2.39}$$

with N_A and N_D the concentration of acceptors and donors and n_i the intrinsic charge carrier concentration. The current voltage characteristics is described by the Shockley-equation:

$$I = eA \left(\sqrt{\frac{D_p}{\tau_p}} \frac{n_i^2}{N_D} + \sqrt{\frac{D_n}{\tau_n}} \frac{n_i^2}{N_A} \right) \left(e^{eV/k_B T} - 1 \right) \tag{2.40}$$

wit A the area, $D_{n/p}$ and $\tau_{n/p}$ the carrier diffusion constants and lifetimes, respectively, and V the external voltage.

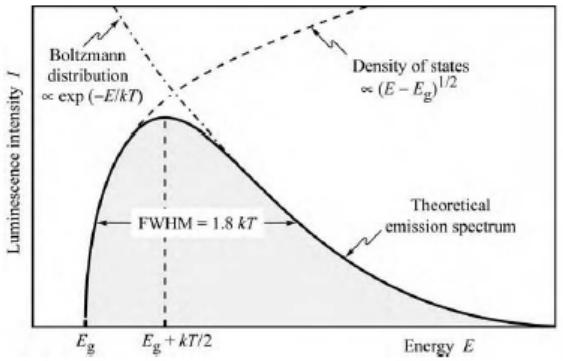

Fig. 5.2. Theoretical emission spectrum of an LED. The full-width at half-maximum (FWHM) of the emission line is $1.8kT$.

Fig. 2.16: Figure from E.F. Schubert "Light emitting diodes" Cambridge University Press (2006).

Under forward bias (diode voltage $V >> k_BT$) we assume that all dopants are ionized and the current can be written as:

$$I = eA\left(\sqrt{\frac{D_p}{\tau_p}}N_A + \sqrt{\frac{D_n}{\tau_n}}N_D\right)\left(e^{e(V-V_D)/k_BT}\right) \tag{2.41}$$

From this, it becomes clear that the current will strongly increase as the voltage V approaches V_D. This defines the threshold voltage $V_{th} \approx V_D \approx E_G/e$ which is also the drive voltage of the LED.

2.3.2.3 Emission characteristics

As for the absorption in solar cells, also for the emission one has to distinguish between direct band gap materials and indirect band gap materials. For recombination, the momentum of the electron and the hole involved has to be the same. In case of an indirect bandgap, a phonon has to be involved in the process to ensure the momentum conservation.
In general, the emission intensity is: $I(E) \propto \sqrt{(E-E_G)}e^{-E/k_BT}$, where $\sqrt{E-E_G}$ describes the DOS of electrons and holes with the same momentum, which can recombine and the Boltzmann factor describes the distribution of charge carriers in the allowed bands.
The maximum emission is at $E = E_G + 1/2k_BT$
The band width of the emission is $\Delta E = 1.8k_BT$ as a result of the derivation of the emission intensity.

2.3.2.4 Efficiencies of LEDs

- Internal quantum efficiency: $\eta_{int} = \frac{P_{int}/h\nu}{I/e}$, i.e. the number of photons emitted from the active region/sec devided by the number of injected electrons/sec.
- Extraction efficiency: $\eta_{extract} = \frac{P/h\nu}{P_{int}/h\nu}$, i.e. the number of photons emitted into free space/sec devided by the the number of photons emitted from the active

region/sec. It is always $\eta_{extract} < \eta_{int}$ due to loss mechanisms (reabsorption, reflection from electrodes).

- External quantum efficiency: $\eta_{ext} = \frac{P/h\nu}{I/e} = \eta_{extract} \cdot \eta_{int}$
- Power efficiency: $\eta_{Power} = \frac{P}{IV}$

White light creation with LEDs

- Combination of several LEDs
- Combining a blue LED with phosphorous (phosphorous emits broad-band yellowish spectrum when illuminated with a blue LED)

Improvements of LED efficiency

- Combination of high mobility materials with highly luminescent materials (especially useful in polymer systems). The high mobility materials acts as transport material, in which the charge carriers also recombine. The excitation energy is then transferred via energy transfer to a highly emissive dye which acts as emitter.
- Lowering of threshold voltage
- Encapsulation to reduce environmental influences and to optimize emission properties

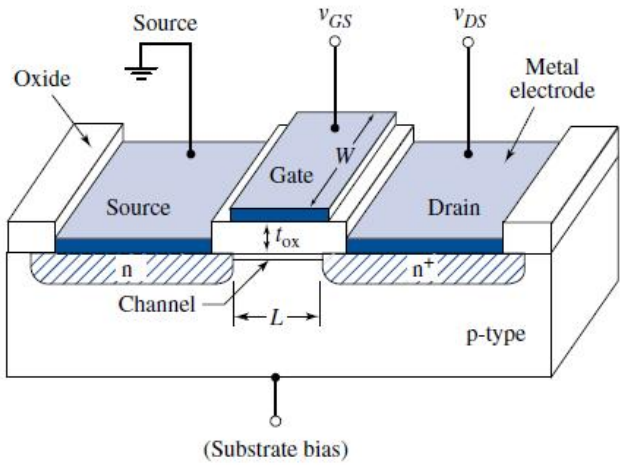

Fig. 2.17: Schematic cross-section through a metal-on-semiconductor field effect transistor [D.A. Neamen, Electronic circuit analysis and design, Mc Graw Hill, 2001]

2.3.3 Field effect transistors

(Following S.M. Sze "Physics of semiconductor devices", John Wiley & Sons, Inc., (1981), and lecture notes by D.A. Wharam and D.P. Kern, University of Tübingen)

Field effect transistors are arguably the most widely spread, archetypal semiconductor devices, forming the basis for electronic devices today as we know them. The most common type is the silicon Metal-Oxide-Semiconductor Field Effect Transistor, or MOSFET, while many other variations exist as well. Some types mark early developments, such as e.g. the JFET (Junction FET), which can be a pn-JFET or a MESFET (Metal-Semiconductor FET). Others are special developments to further improve transistor operation, such as the FINFET (with a fin-shaped channel and a wrap-around gate) or the HEMT (high electron mobility transistor).

The basic principle of the FET, illustrated by a Si-MOSFET, is shown in Fig. 2.17. In this n-channel MOSFET, the bulk material is lightly doped with acceptors (p-type) except for two regions which are called the source and drain. These heavily doped wells define metallic regions in the semiconductor that can be externally connected as ohmic contacts. The key point about the transistor is that at the surface between the semiconductor and the insulating gate oxide, electrons can be induced in the p-type material, and a conductive channel is defined between the source and drain. Conduction through this channel can be tuned by applying a gate voltage V_{GS} to the top gate, which serves to attract electrons to the interface. In this low-dimensional device the electronic states confined within the channel form a (quasi-)2D electron gas, the low-temperature properties of which can demonstrate typical phenomena of mesoscopic physics.

Depending on the transistor configuration, the channel can be *self-conducting* or *self-locking*. In the first case, current flow is enabled even without the application of a gate voltage, and a negative gate voltage needs to be applied to block the channel. In the second case, no conducting channel is present at $V_{GS} = 0\,\mathrm{V}$, and a positive gate voltage needs to be applied to form the channel. Analogously, either electrons or holes can be used as the majority carriers. Correspondingly the type of doping and the polarity of

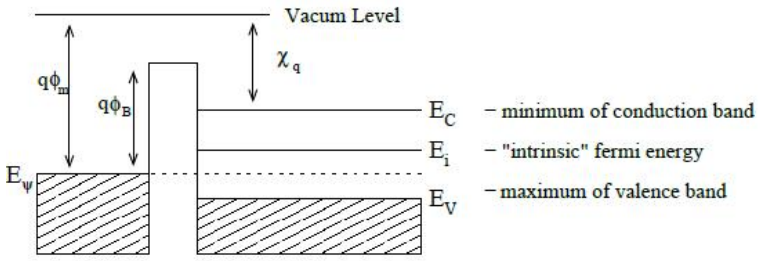

Fig. 2.18: Schematic band structure of the MOSFET under flat-band conditions $V_{GS} = 0$

the gate voltage need to be reversed.
Each of the four combinations (self-conducting / self-locking, electron / hole conduction) leads to comparable typical current-voltage characteristics, however mirrored to different quadrants of the I-V-diagram.

Band structure

First the **linear response regime** with source-drain-voltage $V_{DS} \to 0\,\mathrm{V}$ is considered. Under the assumption that there are no or few surface states, flat band conditions are expected in the absence of a gate bias V_{GS} at any point along the channel (see Fig. 2.18). No band bending is observed.

$q\Phi_m$: Work function - the energy required to remove an electron (from the Fermi surface) of the metal to infinity (surface property)

χ_q: Electron affinity - the energy obtained by moving an electron from the vacuum level to the bottom of the conduction band

E_i: Intrinsic Fermi energy (equidistant between the minimum of the conduction band E_C and the maximum of the valence band E_V)

$q\Phi_B$: Barrier height of the oxide-insulator (i.e. bottom of conduction band in the insulator)

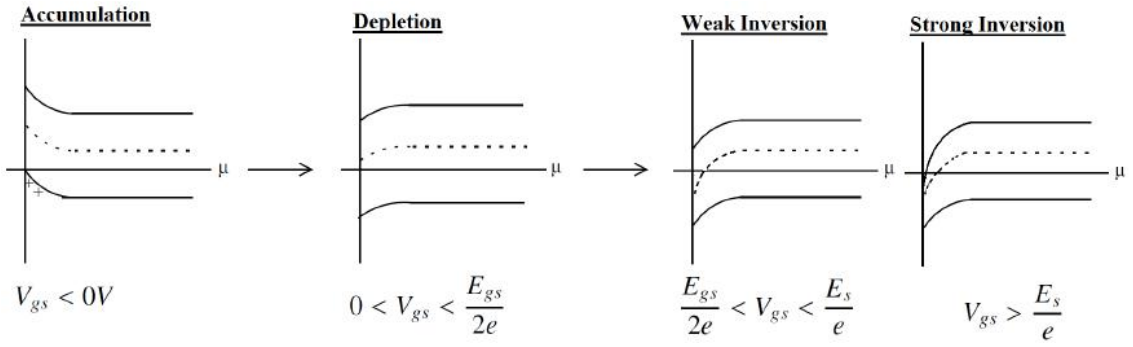

Fig. 2.19: Hole accumulation, depletion, weak inversion, or strong inversion (electron accumulation) conditions depending on the applied gate voltage V_{gs}

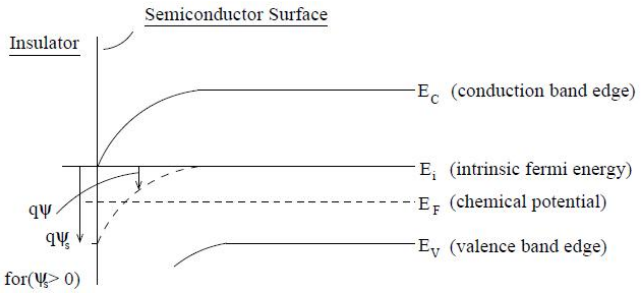

Fig. 2.20: Key parameters of the band structure and position-dependent potential $\psi(x)$

Applying a gate voltage

For gate voltages $V_{GS} < 0\,\mathrm{V}$ the chemical potential of the metal is expected to shift upwards. This leads to band bending and an *accumulation* of charge (holes) within the channel as shown in Fig. 2.19. "Accumulation" applies when the induced carriers are of the same species as given by the doping.

For intermediate positive gate voltages $V_{GS} \geq 0\,\mathrm{V}$ a *depletion* is expected, i.e. a decrease of the number of holes in combination with no significant increase of the electron concentration. This depletion evolves into a *weak inversion* when the intrinsic Fermi energy drops below the chemical potential, and *strong inversion* when the conduction band drops below the chemical potential.

The dependence of bend bending on the gate voltage is schematically shown in Fig. 2.19.

Calculation of the band structure in a MOSFET

To solve the electrostatic MOSFET band structure, an additional position-dependent potential $\psi(x)$ is introduced as shown in Fig. 2.20, which describes the band-bending, i.e. $E_{C,V} = E_{C,V}(\infty) + \psi(x)$. Assuming non-degenerate Fermi statistics, this leads to position-dependent carrier concentrations $n_C(x)$ for the electrons in the conduction band and $p_V(x)$ for the holes in the valence band (charge $e > 0$ and N_{C0}, P_{V0} the bulk concentrations of electrons or holes at the interface):

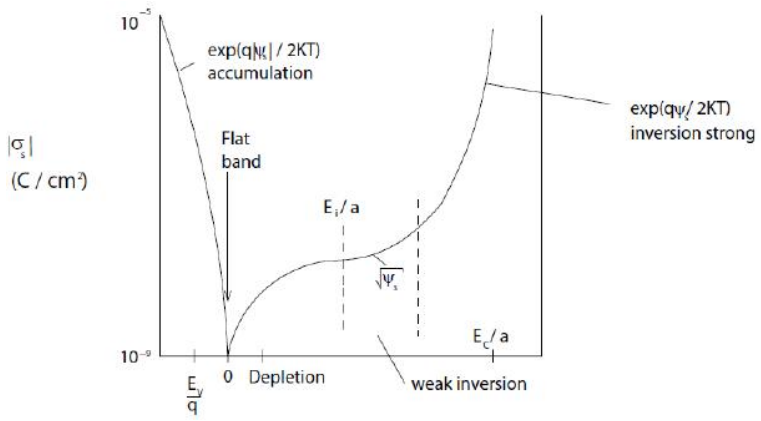

Fig. 2.21: Surface charge density as a function of the surface potential ψ_S

$$n_C(x) = N_{C0}e^{e\psi/k_BT} \quad \text{and} \quad p_V(x) = P_{V0}e^{-e\psi/k_BT} \tag{2.42}$$

with the Boltzmann constant k_B and temperature T. To find a value for the surface potential $\psi_S = \psi(x = 0)$ ("gate voltage"), the Poisson equation is solved using the position-dependent total charge density $\rho(x) = q(N_D^+ - N_A^- + p_V - n_C)$, where N_D^+ and N_A^- are the densities of the ionized donors and acceptors:

$$\frac{d^2\psi}{dx^2} = -\frac{\rho(x)}{\epsilon_r\epsilon_0} \tag{2.43}$$

By taking into account the boundary conditions $\rho(x) = 0$ and $\psi(x) = 0$ for $x \to \infty$ in the bulk ($N_D^+ - N_A^- = N_{C0} - P_{V0}$), the Poisson equation

$$\frac{d^2\psi}{dx^2} = -\frac{e}{\epsilon_r\epsilon_0}\Big(P_{V0}(e^{-\beta\psi} - 1) - N_{C0}(e^{\beta\psi} - 1)\Big) \tag{2.44}$$

with $\beta = \frac{e}{k_BT}$ can be solved for F where $F = -\frac{\partial\psi}{\partial x}$ is the field strength:

$$F^2 = (-\frac{\partial\psi}{\partial x})^2 = \frac{2qP_{V0}}{\beta\epsilon_r\epsilon_0}\Big((e^{-\beta\psi} + \beta\psi - 1) + \frac{N_{C0}}{P_{V0}}(e^{\beta\psi} - \beta\psi - 1)\Big) \tag{2.45}$$

This equation needs to be solved numerically for the surface field strength $F_S = F(x = 0)$ from $F(\psi_S)$, and yields the surface charge density

$$\sigma_S = -\epsilon_r\epsilon_0 F_S \tag{2.46}$$

The change in the surface charge density as a function of ψ_S is shown in Fig. 2.21. Typical surface charges for Si-MOSFETs are $\sim 4 \cdot 10^{16}$ m^{-2}, which together with $\epsilon_r = 12$ yields surface fields $F_S \sim 4 \cdot 10^6$ Vm^{-1} and surface potentials on the order of 1 V.

This steep confinig potential leads to a quantum well with a width on the order of 10 nm at the interface, and thus a 2D electron gas at low temperatures. The roughly triangular quantum well can be modeled by the potential

$$V(z) = \infty \quad \forall\, z < 0 \quad \text{and} \quad V(z) = eFz \quad \forall\, z \geq 0 \tag{2.47}$$

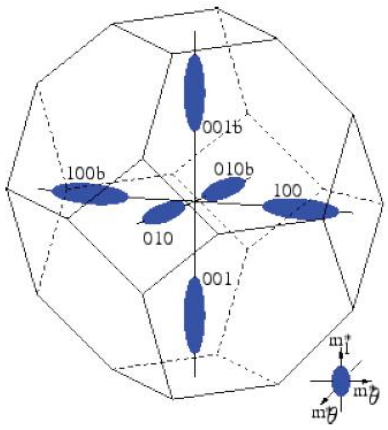

Fig. 2.22: Conductance valleys in the first Brillouin zone of silicon [Dissertation Siddhartha Dhar, TU Wien (2007)]

where z is the spatial coordinate perpendicular to the interface at $z = 0$ pointing in the direction of the semiconductor material.

The solutions of the corresponding Schrödinger equation are given by *Airy functions* with eigenenergies

$$E_n \simeq \left(\frac{\hbar^2}{2m_z}\right)^{1/3}\left(\frac{3\pi eF}{2}(n+\frac{3}{4})\right)^{2/3} \quad \text{with} \quad n \in \mathbb{N} \tag{2.48}$$

Reminder: The band structure of silicon exhibits six valleys in the 1^{st} Brillouin zone, as shown in Fig. 2.22. In the present 2D case, the band structure is projected onto a 2D quantum well, where the two valleys of Si with large effective masses m_z (for Si (100)) have the smallest quantised energies, and the system has an isotropic dispersion in the 2D plane, i.e. $m_x = m_y = 0.19\, m_0$ and $m_z = 0.92\, m_0$.

More realistically, additional terms need to be included in the confining potential taking into account dopant charges, the self-consistent electronic charge distribution, and effective image charges in the oxide. The equation then has to be solved numerically.

Current-voltage characteristics

Figures 2.23 and 2.24(a) show typical current-voltage characteristics of a MOSFET for different fixed values of the gate voltage V_{GS} and a continuous variation of the source-drain voltage V_{DS}. The current increases nearly linearly for low voltages and saturates at a V_{GS}-dependent value of V_{DS}. Connecting the values of saturation displays a roughly parabolic increase of the saturation current $I_{sat}(V_{DS})$.
Figure 2.24(b) shows the transfer characteristics for different fixed values of V_{DS} and a continuous variation of V_{GS}. In the gate voltage range of the slope, the curves coincide before reaching different source-drain-voltage dependent saturation values.
In Figure 2.25 the four different types of MOSFET (n-type *vs.* p-type and self-conducting (depletion type) *vs.* self-locking (enhancement type)) are depicted.

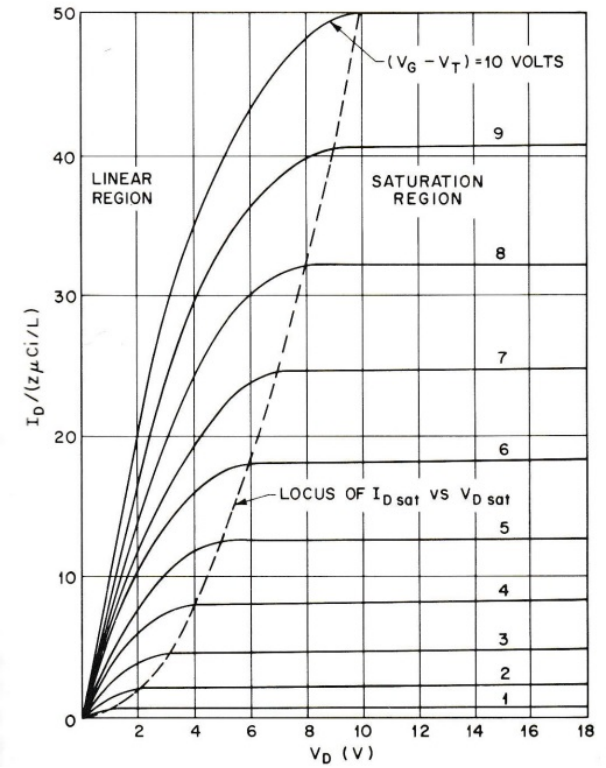

Fig. 2.23: Idealized voltage characteristics $I(U_D)$ of a MOSFET indicating the parabolic shape of the saturation curve (dashed line) connecting the saturation voltages after which the current remains constant [S.M. Sze, John Wiley & Sons, Inc., (1981)]

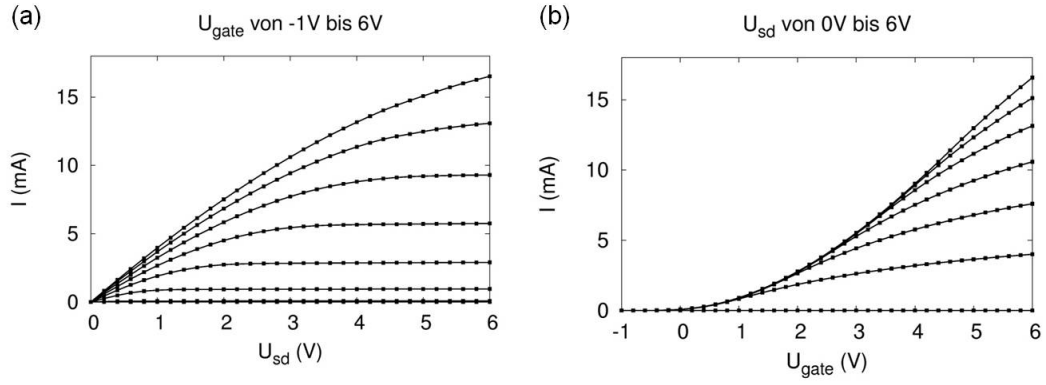

Fig. 2.24: (a) Gate voltage characteristics $I(U_{sd})$ for different fixed values of U_{gate} and (b) transfer characteristics $I(U_{gate})$ for different fixed values of U_{sd} of a MOSFET fabricated in the Advanced Semiconductor Lab Course in Tübingen

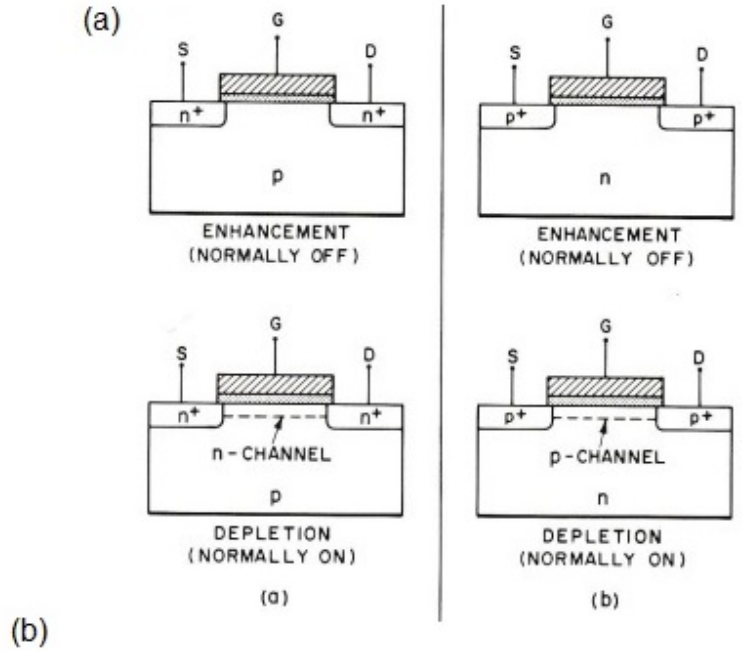

(b)

TYPE	ELECTRICAL SYMBOL	OUTPUT CHARACTERISTIC	TRANSFER CHARACTERISTIC
N-CHANNEL ENHANCEMENT (NORMALLY OFF)		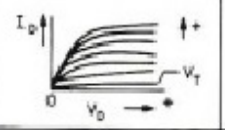	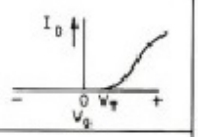
N-CHANNEL DEPLETION (NORMALLY ON)	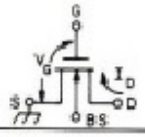	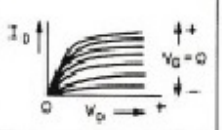	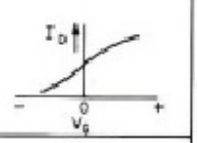
P-CHANNEL ENHANCEMENT (NORMALLY OFF)		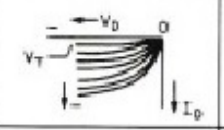	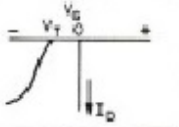
P-CHANNEL DEPLETION (NORMALLY ON)		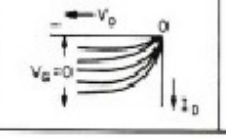	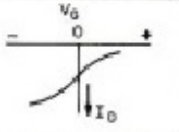

Fig. 2.25: Electric symbols, output characteristics and transfer characteristics of the four types of MOSFET (n-channel vs. p-channel and depletion vs. enhancement) [S.M. Sze, John Wiley & Sons, Inc., (1981), after Gallagher and Corak]